

International
Progress Report

IPR-99-25

Äspö Hard Rock Laboratory

Prototype Repository

Mechanical properties of the diorite in the
prototype repository at Äspö HRL

Laboratory tests

Erling Nordlund, Chunlin Li, Bo Carlsson

Division of Rock Mechanics
Luleå University of Technology

June 1999

Svensk Kärnbränslehantering AB

Swedish Nuclear Fuel
and Waste Management Co
Box 5864
SE-102 40 Stockholm Sweden
Tel 08-459 84 00
+46 8 459 84 00
Fax 08-661 57 19
+46 8 661 57 19



**Äspö Hard Rock
Laboratory**

| | |
|------------------------------|------------|
| Report no. | No. |
| IPR-99-25 | F63K |
| Author | Date |
| E Nordlund, C Li, B Carlsson | June, 1999 |
| Checked by | Date |
| L-O Dahlström, C Svemar | 1999-06-03 |
| Approved | Date |
| Olle Olsson | 1999-11-24 |

Äspö Hard Rock Laboratory

Prototype repository

Mechanical properties of the diorite in the prorotype repository at Äspö HRL

Laboratory tests

Erling Nordlund, Chunlin Li, Bo Carlsson

Division of Rock Mechanics
Luleå University of Technology

June 1999

Keywords: Strength, Young's modulus, Poisson's ratio, fracture toughness
acoustic emission

This report concerns a study which was conducted for SKB. The conclusions and viewpoints presented in the report are those of the author(s) and do not necessarily coincide with those of the client.

Abstract

This report summarises the laboratory tests for determining the following mechanical parameters of the diorite in Äspö HRL:

- Uniaxial compressive strength, σ_c
- Tensile strength, σ_t
- Young's modulus, E
- Poisson's ratio, ν
- Cohesion, c
- Friction angle, ϕ
- Strength constants m in the Hoek-Brown failure criterion
- Crack-initiation stress, σ_{ci}
- Crack-damage stress, σ_{cd}
- Tensile fracture toughness, K_{IC} .

Sammanfattning

Rapporten redovisar laboratorie tester där följande mekaniska parametrar för dioriten i Äspö HRL har bestämts:

- Enaxiell tryckhållfasthet, σ_c
- Draghållfasthet, σ_t
- Elasticitetsmodul, E
- Tvärkontraktionstal, ν
- Kohesion, c
- Inre friktionsvinkel, ϕ
- Hållfasthetskonstant m i Hoek-Browns brottkriterium
- Sprickinitieringsspänning, σ_{ci}
- Sprickskadespänning, σ_{cd}
- Brottseghet, K_{IC} .

Contents

| | |
|------------------------------------------------|------------|
| Abstract | i |
| Sammanfattning | i |
| Contents | ii |
| List of Figures | iii |
| List of Tables | iii |
| 1 Introduction | 1 |
| 2 Test methods | 2 |
| 2.1 Uniaxial tests – ISRM method | 2 |
| 2.2 Triaxial tests – ISRM method | 3 |
| 2.3 Brazil tests – ISRM method | 4 |
| 2.4 Three-Point Bending tests – ISRM method | 5 |
| 3 Parameter evaluation | 7 |
| 3.1 Parameters m , c and ϕ | 7 |
| 3.2 Parameters σ_{ci} and σ_{cd} | 9 |
| 4 Test Equipment | 10 |
| 5 Testing | 11 |
| 5.1 The specimens | 11 |
| 5.2 Results | 12 |
| 6 Summary of the results | 16 |
| References | 16 |
| Appendix | 17 |

List of Figures

| | |
|---------------------------------------------------------------------------------------------------------------------------------------------|----|
| Figure 2-1 Test arrangement for uniaxial tests. | 2 |
| Figure 2-2 Methods for calculating Young's modulus and Poisson's ratio from stress-strain curves. | 3 |
| Figure 2-3 Triaxial test (Brady and Brown, 1993). | 4 |
| Figure 2-4 Apparatus for Brazil test (ISRM, 1981). | 5 |
| Figure 2-5 The chevron bend specimen (Ouchterlony, 1988). | 6 |
| Figure 3-1 The strength envelope of a rock sample. A – Brazil test; B – Uniaxial compression test; C, D and E – Triaxial compression tests. | 8 |
| Figure 3-2 The concept of parameters σ_{ci} and σ_{cd} . | 9 |
| Figure 5-1 The flow chart illustrating the procedure for data evaluation. | 14 |
| Figure 5-2 Fitting the experimental data with the H-B criterion. | 15 |
| Figure 5-3 Fitting the experimental data with the M-C criterion. | 15 |
| Figure A-1 The stress-strain curves of specimen C1. | 17 |
| Figure A-2 The stress-strain curves of specimen C6. | 18 |
| Figure A-3 The stress-strain curves of specimen C9. | 19 |
| Figure A-4 Acoustic emission of specimen C1 under uniaxial compression. | 20 |
| Figure A-5 Acoustic emission of specimen C13 under confining pressure of 5 MPa. | 20 |
| Figure A-6 Acoustic emission of specimen C8 under confining pressure of 20 MPa. | 21 |

List of Tables

| | |
|------------------------------------------------------------------------------|----|
| Table 5-1 All the specimens for the tests. | 11 |
| Table 5-2 The test results. | 13 |
| Table 6-1 The mechanical properties (mean value) of the diorite in Äspö HRL. | 16 |

1 Introduction

The work has been focused on the determination of the mechanical properties of the diorite from Äspö HRL. The mechanical properties determined in this study include

- uniaxial compressive strength, σ_c
- tensile strength, σ_t
- Young's modulus, E
- Poisson's ratio, ν
- cohesion, c
- friction angle, ϕ
- strength constant m in the Hoek-Brown failure criterion
- crack-initiation stress, σ_{ci}
- crack-damage stress, σ_{cd}
- tensile fracture toughness, K_{IC} .

The tests carried out for determining the above parameters were uniaxial and triaxial tests, Brazil disc tests and three point bending tests.

2 Test Methods

2.1 Uniaxial Tests – ISRM Method

This method of test is intended to measure the uniaxial compressive strength (σ_c) as well as to determine Young's modulus (E) and Poisson's ratio (ν) of the rock sample (ISRM, 1979).

Test specimens are right circular cylinders having a height to diameter ratio of 2.5. Two pairs of axial and circumferential strain gauges are diametrically glued on the cylindrical surfaces of the specimens. The stress-strain curves are recorded during loading. The load is applied continuously at a constant loading rate such that failure will occur within 5-10 min of loading, alternatively the stress rate shall be within the limits of 0.5-1.0 MPa/s. The test arrangement is illustrated in Figure 2-1.

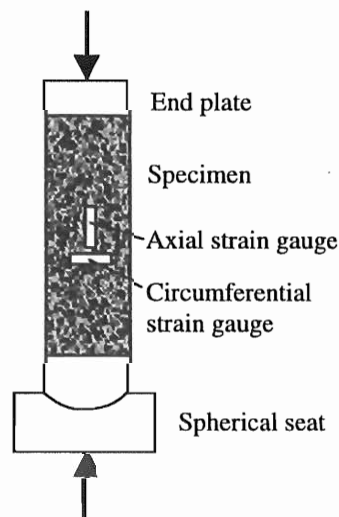


Figure 2-1 Test arrangement for uniaxial tests

The uniaxial compressive strength σ_c is calculated as

$$\sigma_c = \frac{P_{\max}}{A}$$

2-1

where P_{\max} is the ultimate load and A is the area of the cross section of the specimen.

Tangential Young's modulus E is determined at a stress level that is some fixed percentage of the ultimate strength. It is generally evaluated at a stress level equal to

50% of the ultimate strength, denoted as E_{50} . Similarly, the Young's modulus determined at the stress level equal to zero is denoted as E_{ini} . With reference to Figure 2-2, the tangential Young's modulus E and Poisson's ratio ν are calculated as

$$E = \frac{\Delta\sigma_1}{\Delta\varepsilon_1} \quad 2-2$$

$$\nu = -\frac{\Delta\varepsilon_2}{\Delta\varepsilon_1} \quad 2-3$$

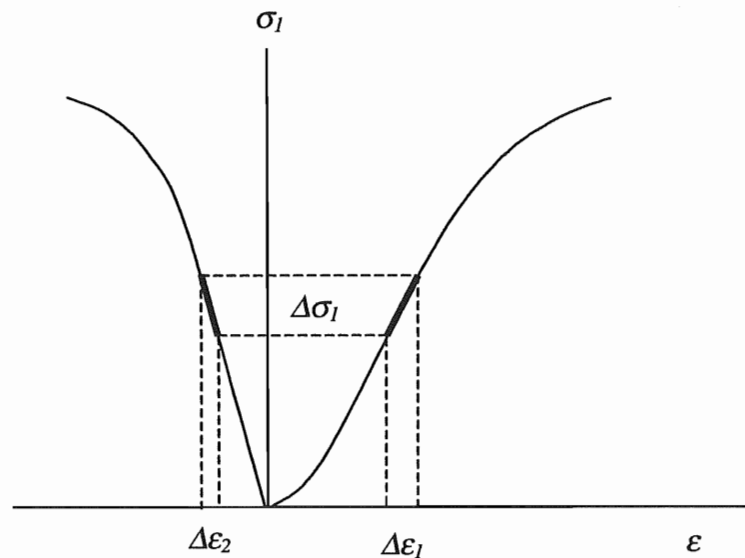
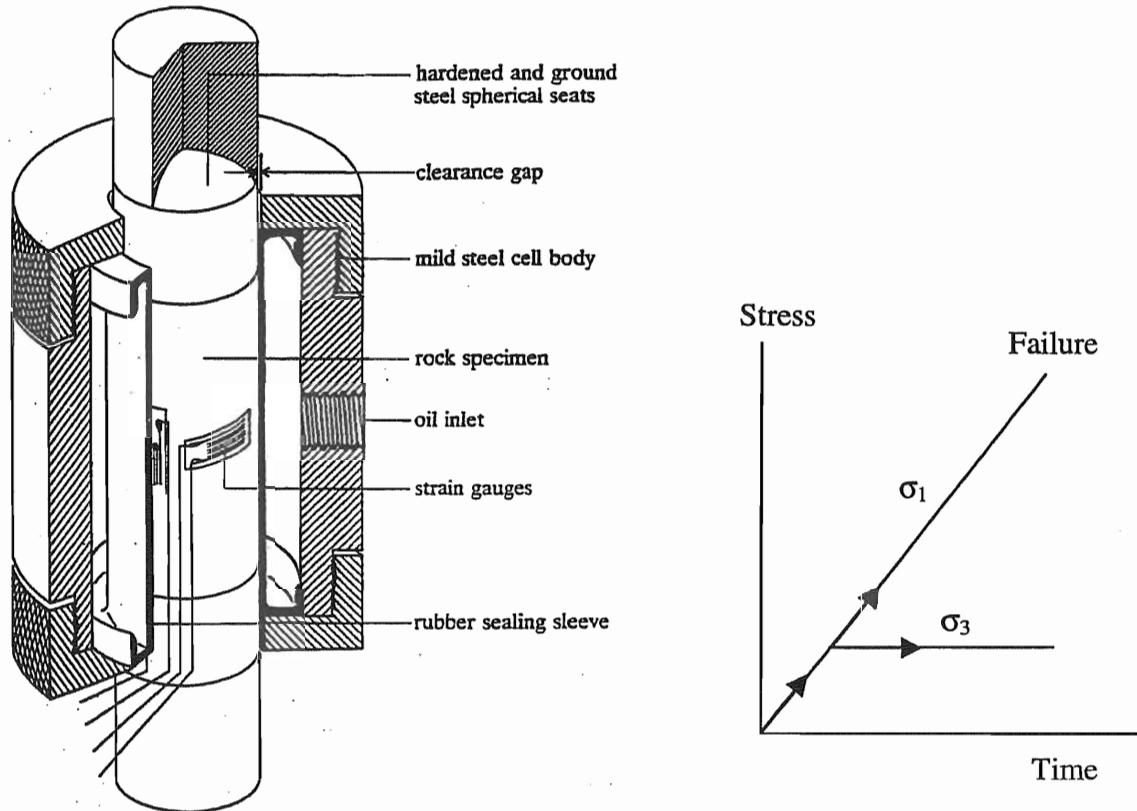


Figure 2-2 Methods for calculating Young's modulus and Poisson's ratio from stress-strain curves.

2.2 Triaxial Tests – ISRM Method

The testing method is intended to measure the compressive strength (σ_{1c}) of a rock sample in presence of a confining pressure (ISRM, 1981). The confining stress is applied through a setup called Hoek cell, Figure 2-3. The cylindrical specimen is wrapped with a rubber sleeve. The space between the rubber sleeve and the steel cell body forms the oil chamber. The pressure in the oil chamber, controlled by a pump, is applied to the spherical surface of the specimen through the sleeve. The axial load is applied in the same way as in the uniaxial compressive tests. The ultimate compressive load at failure is used to determine the strength of the specimen.



(a) Cut-away view of the cell

(b) The loading path

Figure 2-3 Triaxial test (modified after Brady and Brown, 1993).

2.3 Brazil Tests – ISRM Method

The Brazil test is used to determine the uniaxial tensile strength of rock specimens indirectly (ISRM, 1981). The justification for the test is based on the experimental fact that disc rock samples under diametrical loading fail in tension at their tensile strength (Mellor and Hawkes, 1971). The apparatus for Brazil test is illustrated in Figure 2-4. The tensile strength of the specimen, σ_t , is calculated by the following formula:

$$\sigma_t = 0.636 \frac{P}{DT} \quad 2-4$$

where P is the load at failure, D is the diameter of the specimen, and t is the thickness of the specimen.

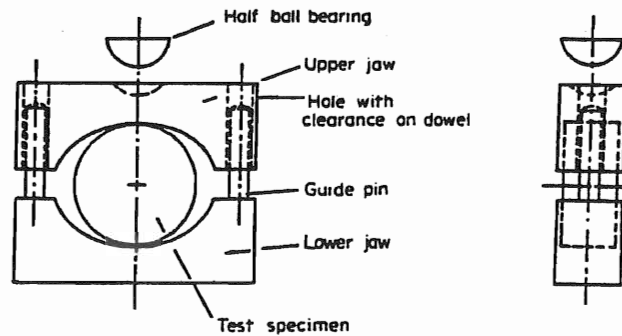


Figure 2-4 Apparatus for Brazil test (ISRM, 1981).

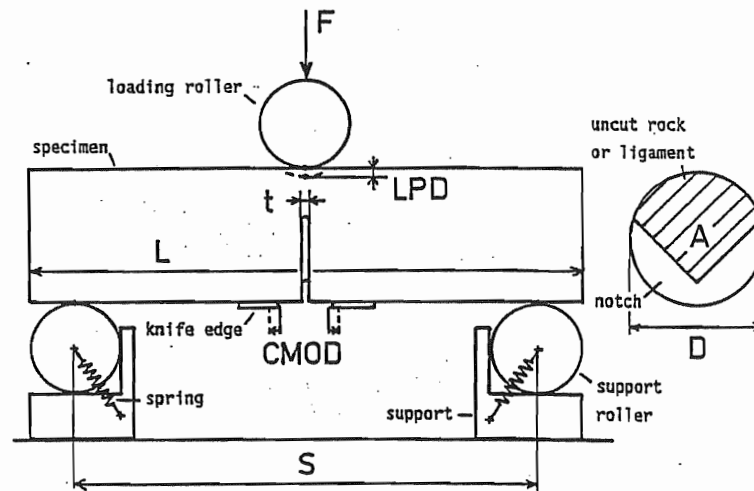
2.4 Three-Point Bending Tests – ISRM Method

This test is used to determine the tensile fracture toughness K_{IC} of rock material (Ouchterlony, 1988). A core specimen, called the chevron bend specimen, with a chevron or V-shaped notch cut perpendicular to the core axis is used in the test, see Figure 2-5. The test has two levels. Level I testing requires only the recording of maximum load. Level II testing requires continuous load and displacement measurements to be made during the test. We only ran Level I test. The fracture toughness K_{IC} is calculated by the following formulae:

$$K_{IC} = A_{\min} F_{\max} / D^{1.5} \quad 2-5$$

$$A_{\min} = \left[1.835 + 7.15 \frac{a_0}{D} + 9.85 \left(\frac{a_0}{D} \right)^2 \right] \frac{S}{D} \quad 2-6$$

where F_{\max} is the ultimate load at failure, D the diameter of the specimen, S the distance between support points, and a_0 the chevron tip distance from the specimen surface.



Basic notation:

- D = diameter of chevron bend specimen
- S = distance between support points, $3.33 \cdot D$
- θ = chevron angle, 90°
- a_0 = chevron tip distance from specimen surface, $0.15 \cdot D$.
- a = crack length
- t = notch width
- h = depth of cut in notch flank
- L = specimen length
- A = projected ligament area
- F = load on specimen
- LPD = deflection of load point relative to support points
- CMOD = relative opening of knife edges

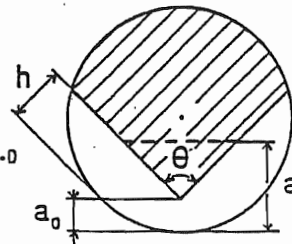


Figure 2-5 The chevron bend specimen (Ouchterlony, 1988).

3 Parameter Evaluation

3.1 Parameters m , c and ϕ

Based on the results of the uniaxial, triaxial and Brazil tests, the strength of the rock sample can be plotted in a σ_1 - σ_3 diagram as shown in Figure 3-1. The strength envelope can be either fitted by the Hoek-Brown (H-B) failure criterion, expressed as:

$$\sigma_1 = \sigma_3 + \sqrt{m\sigma_c\sigma_3 + \sigma_c^2} \quad 3-1$$

or by the Mohr-Coulomb (M-C) failure criterion, expressed as:

$$\sigma_1 = k\sigma_3 + C \quad 3-2$$

where

$$k = \frac{1 + \sin \phi}{1 - \sin \phi}, \quad 3-3$$

$$C = \frac{2c \cos \phi}{1 - \sin \phi}, \quad 3-4$$

c and ϕ represent the cohesion and friction angle of the material, respectively.

Using the H-B criterion, we can obtain a fitting curve to the experimental data by selecting an appropriate value for parameter m in Eq. (3-1), see Figure 3-1.

Similarly using the M-C criterion, parameters k and C can be obtained by linear regression of the test results of the uniaxial and triaxial tests. The cohesion c and the friction angle ϕ are then obtained from Eqs. (3-3) and (3-4).

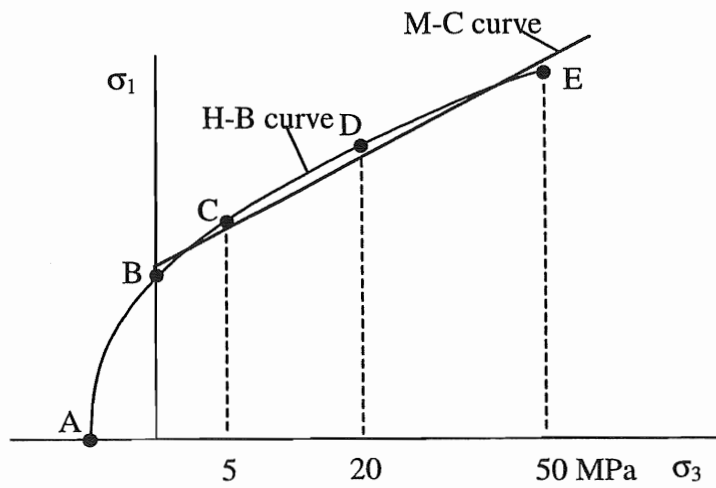


Figure 3-1 The strength envelope of a rock sample. A – Brazil test; B – Uniaxial compression test; C, D and E – Triaxial compression tests.

3.2 Parameters σ_{ci} and σ_{cd}

The failure of competent rocks under compressive loading is progressive. It has been observed through specific monitoring techniques, for instance the acoustic emission technique, that the failure of rock starts at quite low stress levels in the form of stable cracking. Based on the variation of the volumetric strain during loading, Martin and Chandler (1994) identified two characteristic stress levels marking different stages of cracking (see Figure 3-2). The first one is termed the crack-initiation stress (σ_{ci}). Cracks are thought to start to propagate in a stable manner when the stress reaches the level of σ_{ci} . That means that cracks will not propagate further unless load is increased in the stable propagation stage. σ_{ci} corresponds to the onset of the dilation of the *purely crack-induced volumetric strain*. Another characteristic stress level is termed the crack-damage stress (σ_{cd}). It is defined as the stress level at which the dilation of the *total volumetric strain*, including the elastic component, begins. Above the level of σ_{cd} , it is thought that cracks propagate in an unstable manner, that is, cracks can continue to propagate without increase in load. Rock can not sustain loads permanently above this level. σ_{cd} is actually the creeping strength of material.

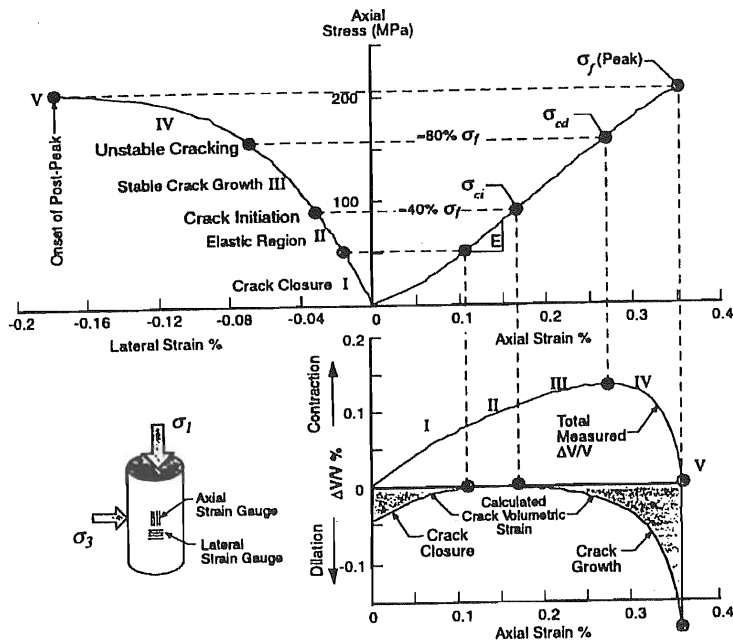


Figure 3-2 The concept of parameters σ_{ci} and σ_{cd} .

4 Test Equipment

The uniaxial and triaxial compressive tests were conducted using the servo-controlled hydraulic testing machine INSTRON 1346. A Hoek cell was used in the triaxial tests to apply the confining pressure. The Brazil tests were conducted using the servo-controlled testing machine, INSTRON 1342. The load and the strain were registered during testing using the computer program LABTECH NOTEBOOK. Acoustic emission (AE) emitted from the specimens during testing was monitored by the AE system MISTRAS. The equipment used in the tests are described in detail in the following.

INSTRON 1346 is a servo-controlled hydraulic testing machine with a Dartec electronic control system. The capacity of the machine is 4500 kN. The load can be applied either under load control or under displacement control. The loading rate can be pre-set with a resolution of 0.0001 kN/s or mm/s.

INSTRON 1342 is another model of the INSTRON testing machine series. The capacity of the machine is 100 kN.

The triaxial Hoek cell looks like that shown in Figure 2-3a. The capacity of confining pressure of the cell is 60 MPa.

MISTRAS is a modern, computerised acoustic emission (AE) equipment, manufactured by Physical Acoustic Corporation. It performs AE signal measurements and stores, displays and analyses the resulting data. The frequency band of the preamplifier is between 100 and 1200 kHz. The threshold and the gain of the post amplifier could be set in the setup menu of the test running code.

5 Testing

5.1 The specimens

The specimens were prepared using the cores from three boreholes drilled in the floor of the tunnel in the Äspö Hard Rock Laboratory. The diameter of the cores is 45 mm. All the specimens are listed in Table 5-1.

Table 5-1 All the specimens for the tests.

| No. | Depth (m) | Borehole | Dimension (mm) Diameter × Length |
|-------------------------------------|--------------|----------|-------------------------------------|
| <u>For compression tests</u> | | | |
| C1 | 1.95 – 2.10 | KA3557G | φ45 × 115 |
| C2 | 2.45 – 2.60 | KA3557G | φ45 × 115 |
| C3 | 2.60 – 2.75 | KA3557G | φ45 × 115 |
| C4 | 2.75 – 2.90 | KA3557G | φ45 × 115 |
| C5 | 3.86 – 4.01 | KA3557G | φ45 × 115 |
| C6 | 5.11 – 5.26 | KA3557G | φ45 × 115 |
| C7 | 5.26 – 5.41 | KA3557G | φ45 × 115 |
| C8 | 7.08 – 7.24 | KA3557G | φ45 × 115 |
| C9 | 7.40 – 7.55 | KA3557G | φ45 × 115 |
| C10 | 1.46 – 1.62 | KA3545G | φ45 × 115 |
| C11 | 1.84 – 2.01 | KA3545G | φ45 × 115 |
| C12 | 2.12 – 2.28 | KA3545G | φ45 × 115 |
| C13 | 3.52 – 3.67 | KA3545G | φ45 × 115 |
| C14 | 3.68 – 3.84 | KA3545G | φ45 × 115 |
| C15 | 3.84 – 3.99 | KA3545G | φ45 × 115 |
| C16 | 4.34 – 4.49 | KA3545G | φ45 × 115 |
| C17 | 6.01 – 6.18 | KA3545G | φ45 × 115 |
| C18 | 4.69 – 4.85 | KA3551G | φ45 × 115 |

Table 5-1 (continued)

| <u>For Brazil tests</u> | | | |
|--------------------------------------|-------------|---------|-----------------------|
| BR1-2(1) | 1.30 – 1.45 | KA3557G | $\phi 45 \times 22.5$ |
| BR1-2(2) | 1.30 – 1.45 | KA3557G | $\phi 45 \times 22.5$ |
| BR3-5(1) | 0.94 – 1.09 | KA3545G | $\phi 45 \times 22.5$ |
| BR3-5(2) | 0.94 – 1.09 | KA3545G | $\phi 45 \times 22.5$ |
| BR3-5(3) | 0.94 – 1.09 | KA3545G | $\phi 45 \times 22.5$ |
| <u>For three point bending tests</u> | | | |
| B1 | 0.54 – 0.74 | KA3557G | $\phi 45 \times 180$ |
| B2 | 0.74- 0.94 | KA3557G | $\phi 45 \times 180$ |
| B3 | 2.10- 2.30 | KA3557G | $\phi 45 \times 180$ |
| B4 | 2.90 – 3.11 | KA3557G | $\phi 45 \times 180$ |
| B5 | 7.44 – 7.64 | KA3545G | $\phi 45 \times 180$ |

5.2 Results

The axial stress-strain curves of three specimens are shown in Figs. A.1-A.3 in the Appendix. The Young's modulus E , Poisson's ratio ν , crack-initiation stress σ_{ci} and crack-damage stress σ_{cd} are evaluated using these curves. The test results of all the specimens are listed in Table 5-2. The procedure for data evaluation is illustrated in the flow chart in Figure 5-1.

Plotting the results of the compression and Brazil tests in Figure 9 and fitting the scatter points by the H-B criterion, we obtain the constant $m = 15$.

Similarly plotting the results of the compression tests in Figure 10 and fitting the scatter points by the M-C criterion, we obtain the cohesion $c = 49$ MPa and the friction angle $\phi = 44^\circ$.

In the Appendix are also the acoustic emission records of three specimens shown, see Figure A.4-A.6. The AE-onset stress is about 50% of the ultimate strength of the rock.

Table 5-2 The test results.

| Compression tests | | | | | | | | | | |
|--------------------------|---------------------|-------------------|------------------------|-----|--------------|----------|-------------|------------|------------------------|------------------------|
| No. | σ_3 (MPa) | P_{max} (kN) | σ_{1c} (MPa) | | E (GPa) | | ν | | σ_{ci} (MPa) | σ_{cd} (MPa) |
| | | | mean | | E_{ini} | E_{50} | ν_{ini} | ν_{50} | | |
| C1* | 0 | 327 | 206 | 219 | 75 | 75 | 0.23 | 0.27 | 147 | 192 |
| C6* | 0 | 365 | 229 | | 86 | 75 | 0.22 | 0.29 | 98 | 195 |
| C9* | 0 | 322 | 202 | | 79 | 70 | 0.19 | 0.27 | 108 | 184 |
| C10 | 0 | 379 | 238 | | | | | | | |
| C7 | 5 | 432 | 272 | 256 | | | | | | |
| C11 | 5 | 411 | 258 | | | | | | | |
| C18 | 5 | 380 | 239 | | | | | | | |
| C5 | 20 | 575 | 362 | 346 | | | | | | |
| C15 | 20 | 556 | 350 | | | | | | | |
| C17 | 20 | 520 | 327 | | | | | | | |
| C4 | 40 | 690 | 434 | 690 | | | | | | |
| C3 | 50 | 723 | 455 | 502 | | | | | | |
| C12 | 50 | 840 | 528 | | | | | | | |
| C16 | 50 | 832 | 523 | | | | | | | |

* strain-gauged specimen;

Dimension: $\phi 45 \times 115$ mm

| Brazil tests | | | |
|---------------------|----------------|------------------------------------|------|
| Specimen No. | Ultimate load | Tensile strength, σ_t (MPa) | |
| | P_{max} (kN) | mean | |
| BR1-2(1) | 25.3 | 15.8 | 14.7 |
| BR1-2(2) | 26.4 | 16.5 | |
| BR3-5(1) | 20 | 12.5 | |
| BR3-5(2) | 23 | 14.4 | |
| BR3-5(3) | 23 | 14.4 | |

Diameter of the specimens: $D = 45$ mm, Thickness of the specimens: $t = 22.5$ mm

| Three-point bending tests | | | | |
|----------------------------------|----------------------------|---------------------------------|--------------------------------------------------|------|
| Specimen No. | Tip distance a_0 (mm) | Ultimate load F_{max} (kN) | Fracture toughness K_{IC} (MPa \sqrt{m}) | |
| | | | mean | |
| B1 | 7.7 | 2.81 | 3.28 | 3.21 |
| B2 | 7.2 | 2.92 | 3.29 | |
| B3 | 7.5 | 2.60 | 3.00 | |
| B4 | 7.4 | 2.94 | 3.36 | |
| B5 | 7.7 | 2.69 | 3.14 | |

 $D = 45$ mm, $S = 3.33D = 150$ mm.

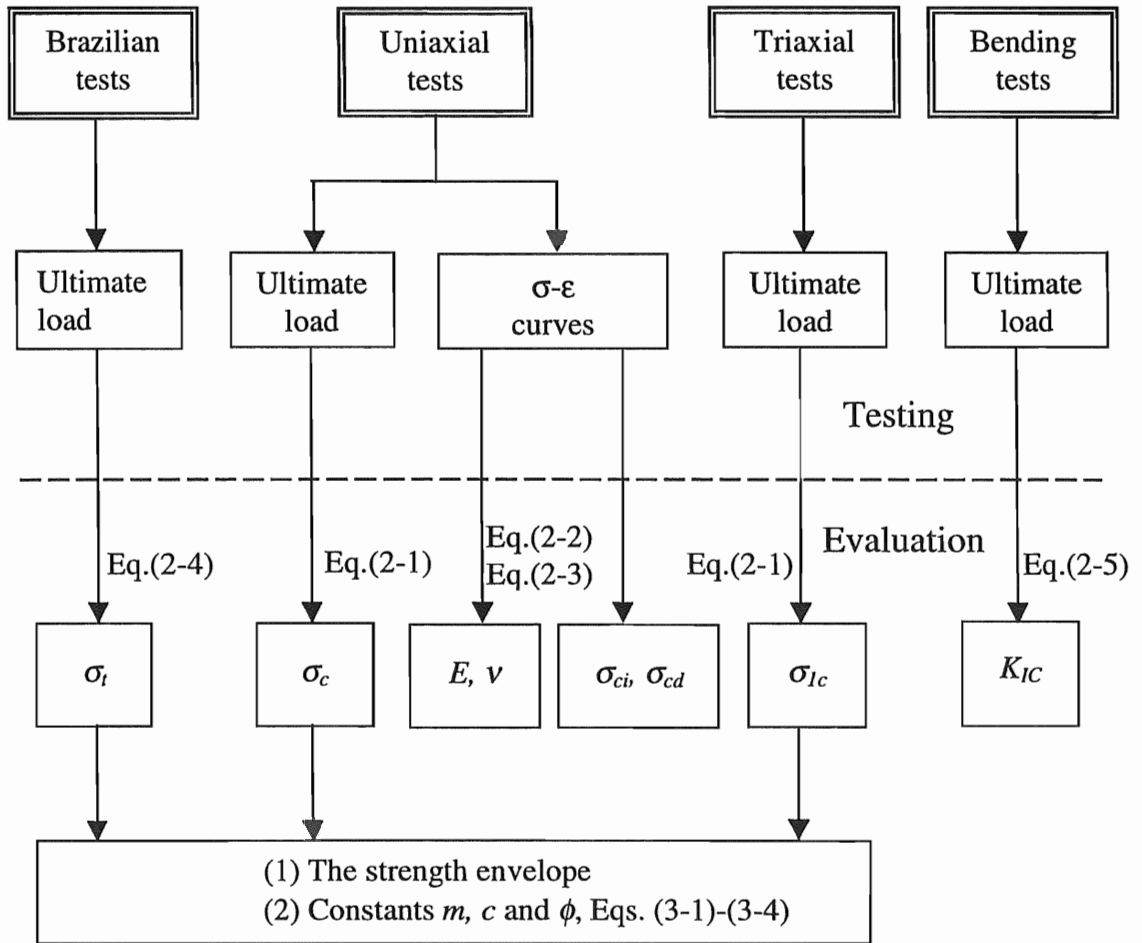


Figure 5-1 The flow chart illustrating the procedure for data evaluation.

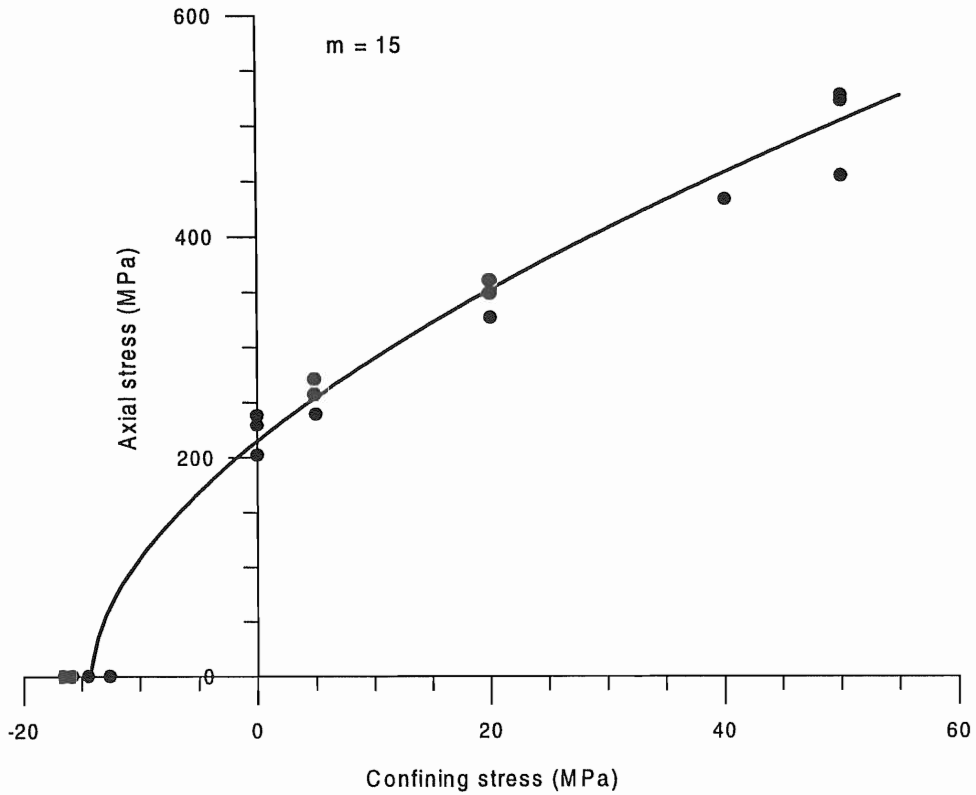


Figure 5-2 Fitting the experimental data with the H-B criterion.

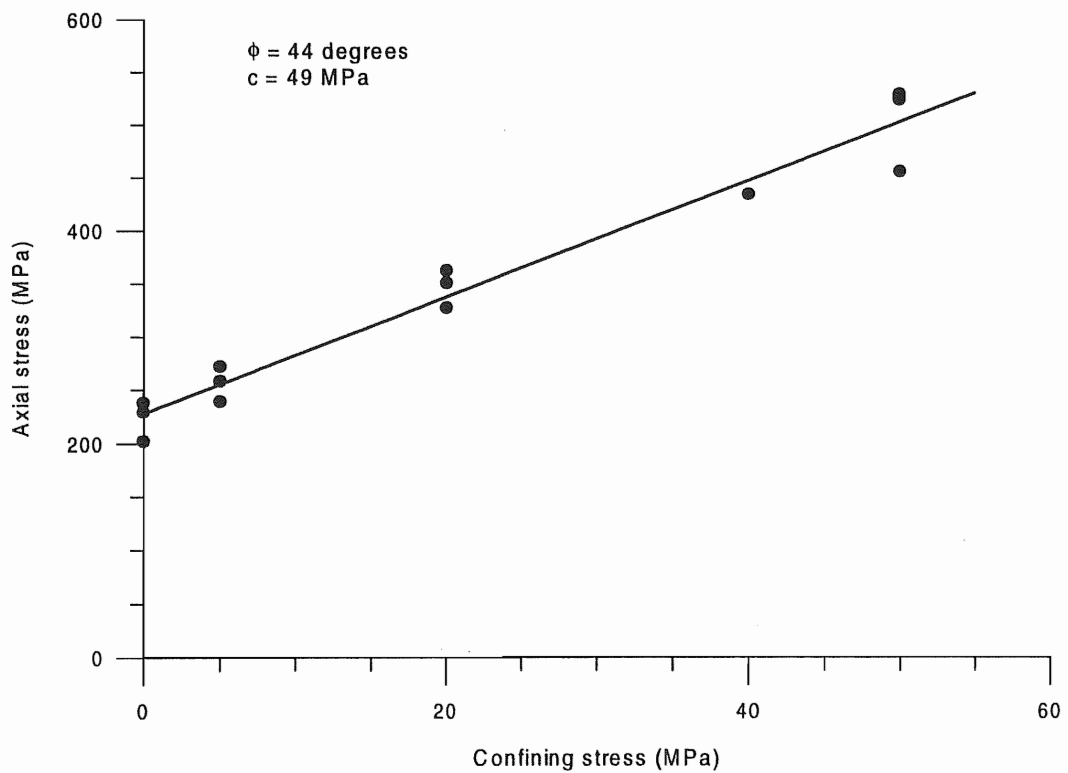


Figure 5-3 Fitting the experimental data with the M-C criterion.

6 Summary of the Results

Table 6-1 The mechanical properties (mean value) of the diorite in Äspö HRL.

| Parameter | value | Unit |
|-------------------------------------------|-------|----------------|
| Uniaxial compressive strength, σ_c | 219 | MPa |
| Tensile strength, σ_t | 14.7 | MPa |
| Young's modulus, E_{ini} | 80 | GPa |
| Young's modulus, E_{50} | 73 | GPa |
| Poisson's ratio, ν_{ini} | 0.21 | |
| Poisson's ratio, ν_{50} | 0.28 | |
| Tensile fracture toughness, K_{IC} | 3.21 | MPa \sqrt{m} |
| Cohesion, c | 49 | MPa |
| Friction angle, ϕ | 44° | |
| H-B criterion constant, m | 15 | |
| Crack-initiation stress, σ_{ci} | 118 | MPa |
| Crack-damage stress, σ_{cd} | 190 | MPa |

References

Brady, B. H. G., and Brown, E. T. 1993. Rock Mechanics for Underground Mining. Chapman & Hall.

ISRM 1979. Suggested methods for determining the uniaxial compressive strength and deformability of rock materials. Int. J. Rock Mech. Min. Sci., 16, p135-140.

Brown, E.T. (ed.) 1981. Suggested methods for determining the strength of rock materials in triaxial compression. ISRM Suggested Methods, Pergmon, Oxford, p125-127.

Brown, E.T. (ed.) 1981. Suggested methods for determining tensile strength of rock materials. ISRM Suggested Methods, Pergmon, Oxford, p119-121.

Martin, C. D. and Chandler, N. A. 1994. The progressive fracture of Lac du Bonnet granite. Int. J. Rock Mech. Min. Sci. & Geomech. Abstr. 31(6), p643-659.

Mellor, M. and Hawkes, I. 1971. Measurement of tensile strength by diametral compression of discs and annuli. Engng. Geol. 5, p173-225.

Ouchterlony, F. 1988. Suggested methods for determining the fracture toughness of rock. Int. J. Rock Mech. Min. Sci. & Geomech. Abstr. 25, p71-96.

APPENDIX The stress-strain curves and acoustic emission records

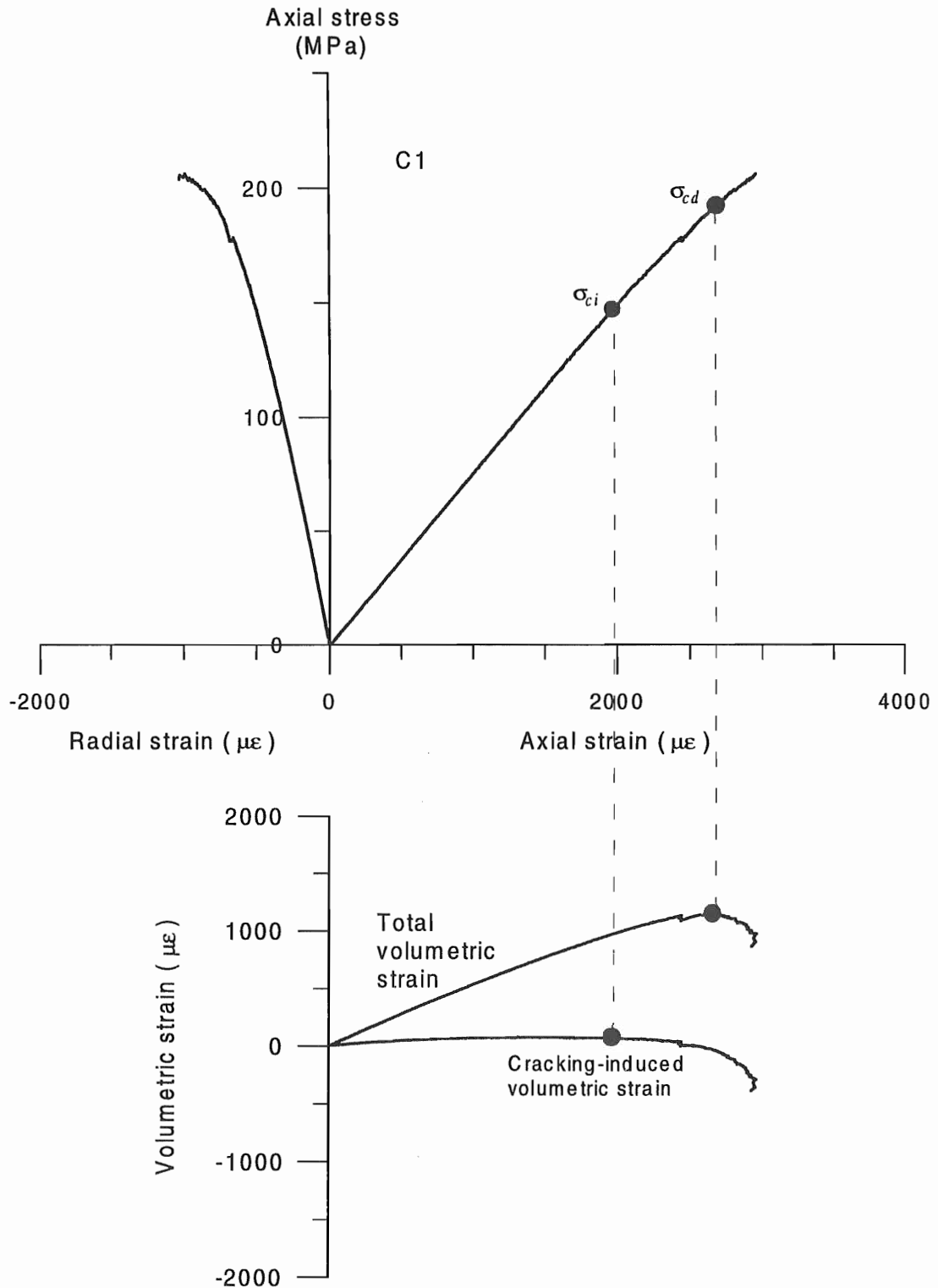


Figure A-1 The stress-strain curves of specimen C1.

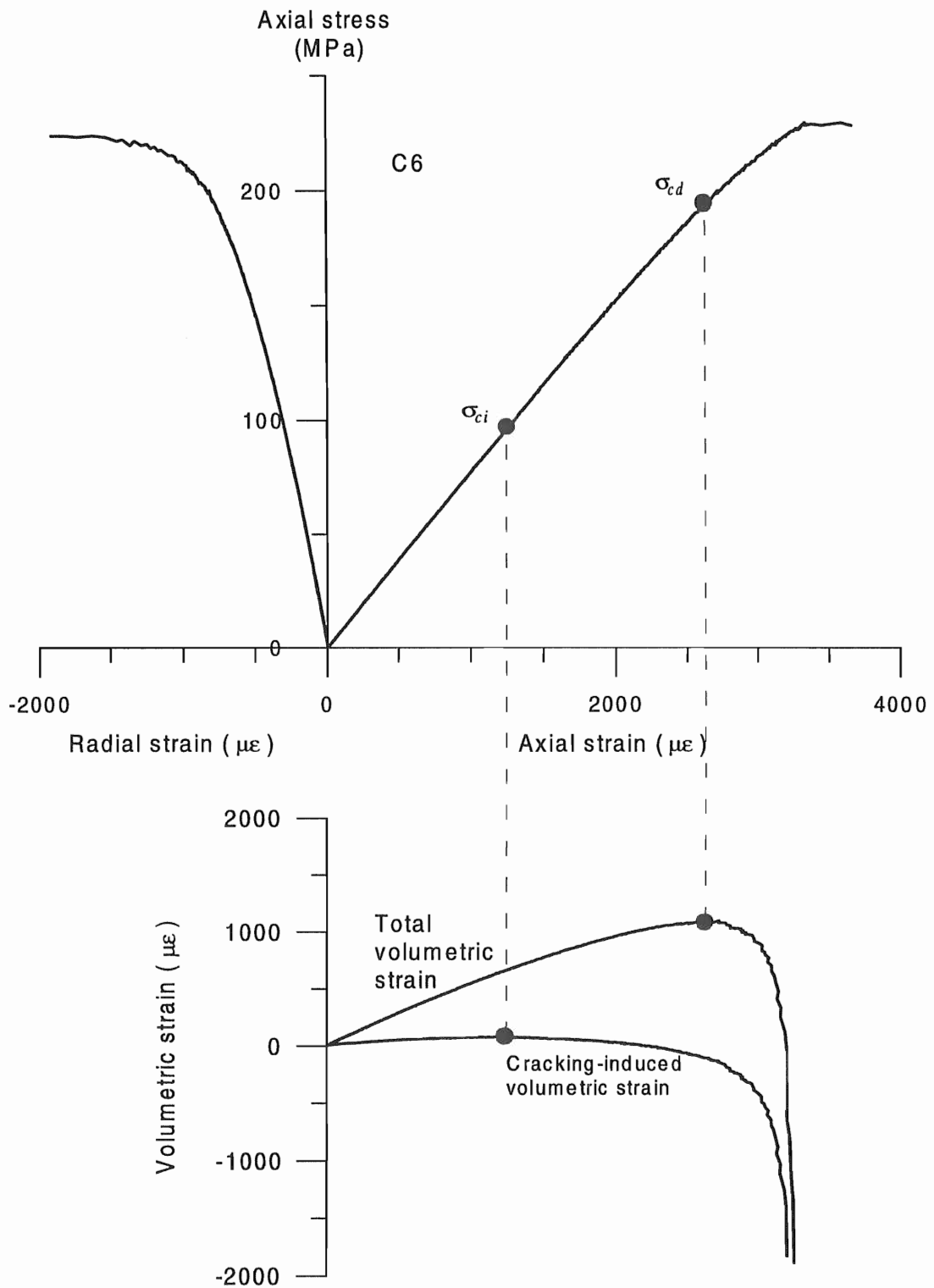


Figure A-2 The stress-strain curves of specimen C6.

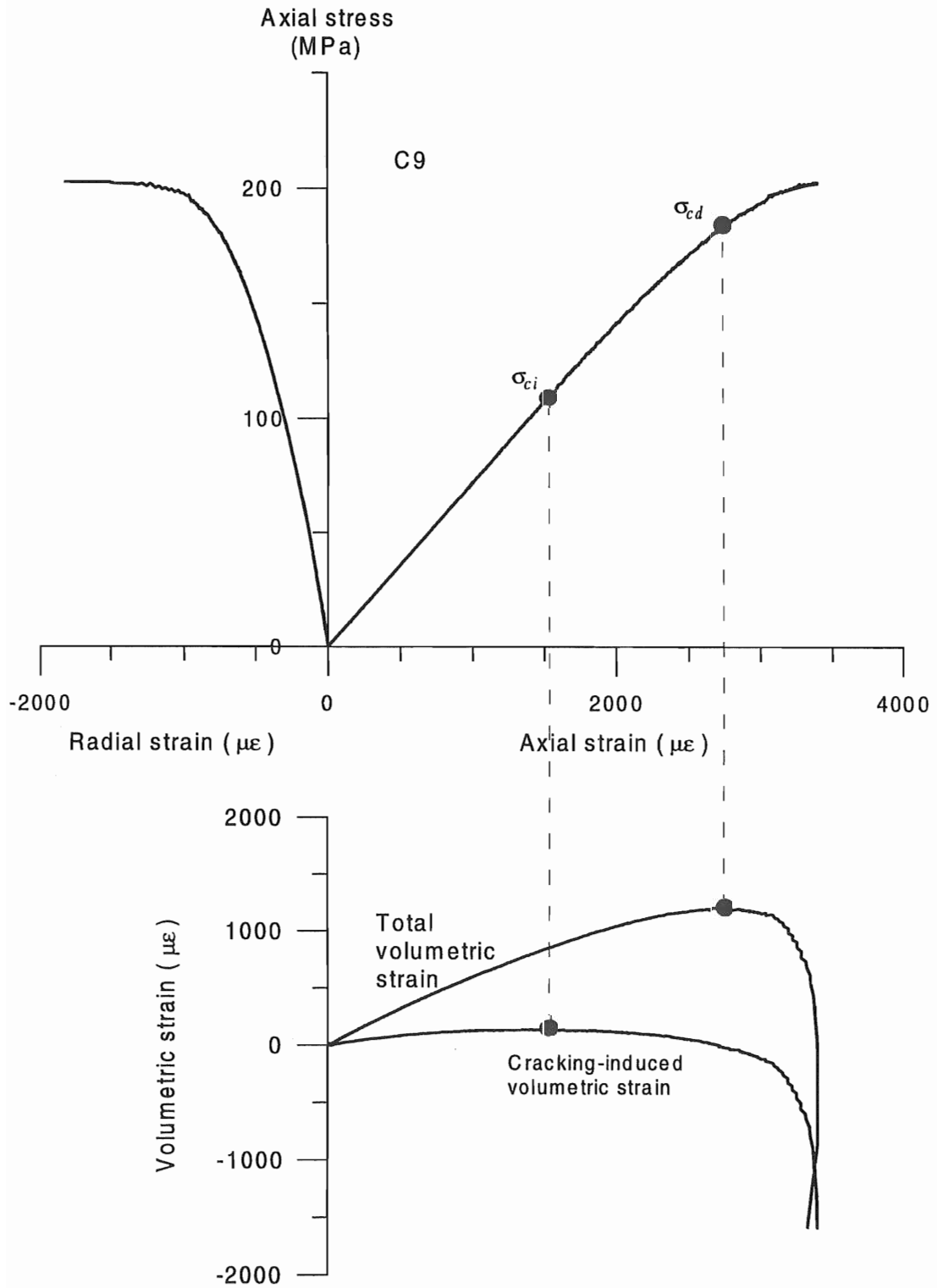


Figure A-3 The stress-strain curves of specimen C9.

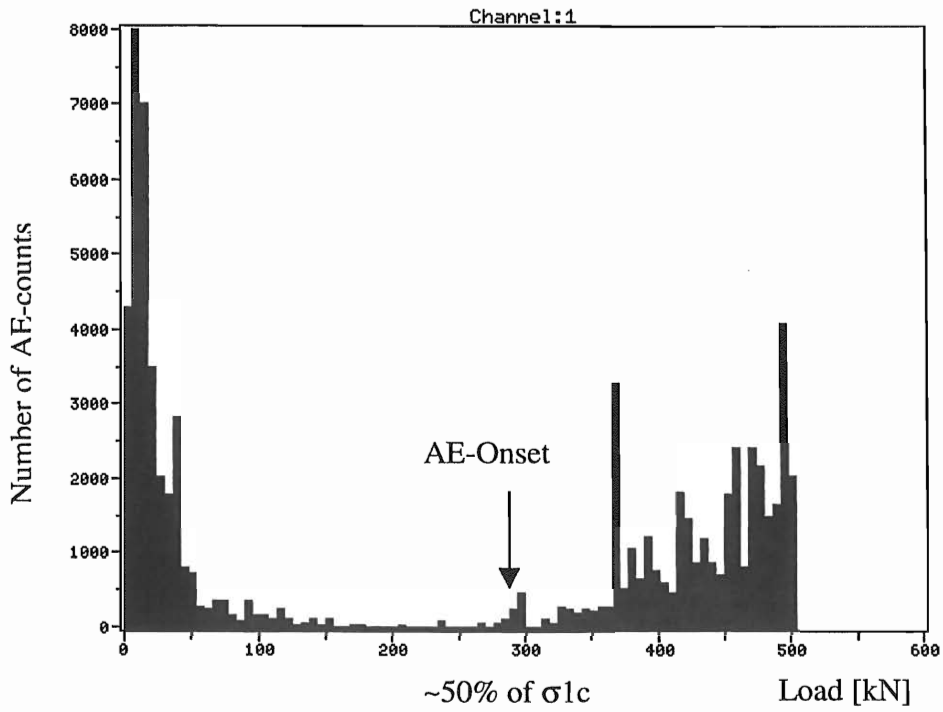


Figure A-4 Acoustic emission of specimen C1 under uniaxial compression.

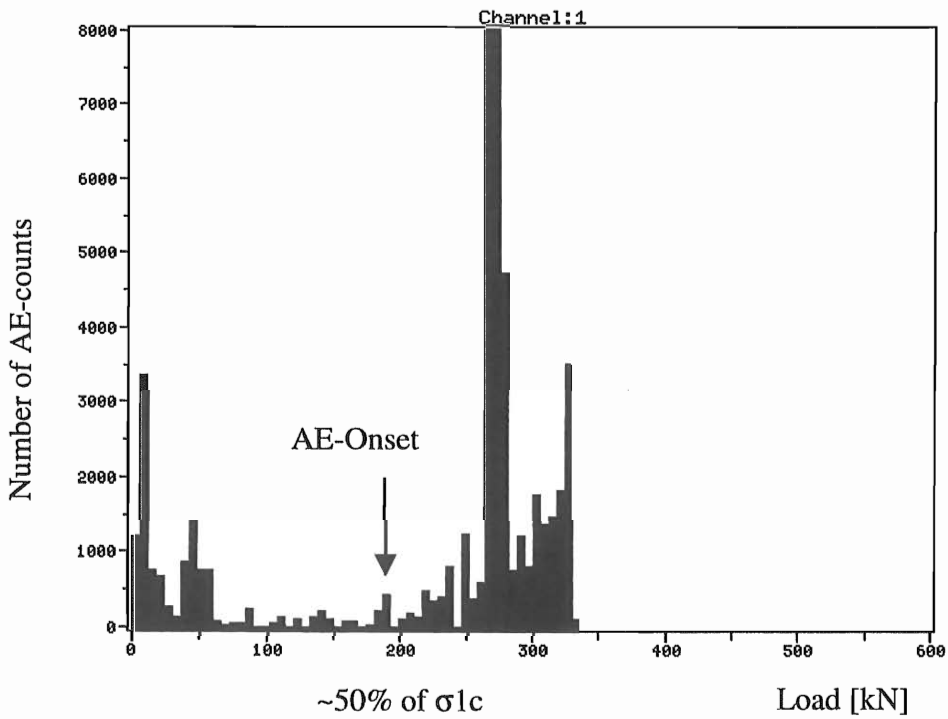


Figure A-5 Acoustic emission of specimen C13 under confining pressure of 5 MPa.

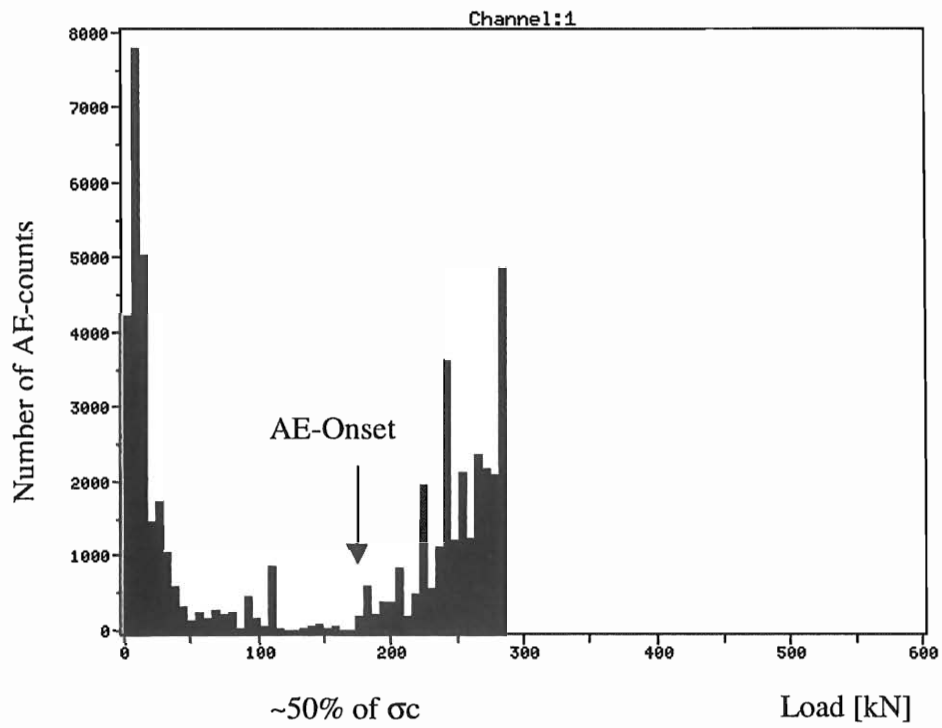


Figure A-6 Acoustic emission of specimen C8 under confining pressure of 20 MPa.